Can small-scale turbulence approach a quasi-universal state?

Shunlin Tang[*]

Institute for Turbulence-Noise-Vibration Interaction and Control, Shenzhen Graduate School,
Harbin Institute of Technology, Shenzhen 518055, China

Robert A. Antonia and Lyazid Djenidi

Discipline of Mechanical Engineering, School of Engineering, University of Newcastle,
Newcastle, 2308 New South Wales, Australia

Yu Zhou

Institute for Turbulence-Noise-Vibration Interaction and Control, Shenzhen Graduate School, Harbin Institute
of Technology, Shenzhen 518055, China
and Digital Engineering Laboratory of Offshore Equipment, Shenzhen, 518055, China

For the past 50 years or so, Kolmogorov's (1962) correction (K62) to his 1941 hypotheses (K41) has been embraced by an overwhelming majority of turbulence researchers. However, we show in this paper that there are no valid reasons for abandoning K41, a similarity framework known for its simplicity and elegance. In particular, analytical considerations, based on the Navier-Stokes equations, which take into account the finite Reynolds number (FRN) effect, together with all available experimental laboratory data, confirm a tendency towards the universal predictions of K41 as the Reynolds number continues to increase. This is especially true when the focus is on the energy spectrum and velocity structure function in the dissipative range. Incorrectly accounting for the FRN effect, which has been almost invariably mistaken for the intermittency effect, and the inclusion of the atmospheric surface layer data are the major factors which have contributed to the heretofore almost unrivalled acceptance of K62.

I. INTRODUCTION

The significant attention that researchers have paid to the properties of small-scale turbulence in different flows and over a range of Reynolds numbers is not surprising given that, from a theoretical viewpoint, small scales are more amenable to being fully understood than the larger scales of the flow. More particularly, the possibility that these properties may become universal, i.e., independent of the Reynolds number as well as the flow, cannot be ruled out, at least for extremely large Reynolds numbers and provided local isotropy is satisfied. In reality, the Reynolds number is usually finite and local isotropy is hardly ever satisfied perfectly. Nonetheless, it is important that we continue to scrutinize the way these properties vary as the Reynolds number increases with the objective of determining whether one can identify regions in various different flows where the departure from local isotropy is small and independent of the Reynolds number. The obvious expectation is that this should be more feasible for dissipative range (DR) than inertial range (IR) properties. We tentatively denote this state as "quasi-universal."

---

[*]shunlin.tang88@gmail.com

The theory of small-scale turbulence has benefited immensely from the contributions of Taylor [1], who introduced the concept of isotropy and obtained a simplified expression for the mean energy dissipation rate $\bar{\epsilon}[=\bar{\epsilon}_{iso} = 15\nu\overline{(\partial u/\partial x)^2}$ if local isotropy is assumed, ν is the kinematic viscosity of the fluid], and Karman and Howarth [2] who derived a transport equation (hereafter referred to as the KH equation) for the two-point velocity correlation function in isotropic turbulence. Further significant progress was made in 1941 when Kolmogorov [3] introduced two important hypotheses, specifically the first and second similarity hypotheses dealing with turbulence scales in the DR and IR at very large Reynolds numbers. In a separate paper, Kolmogorov [4] also derived, starting with the KH equation rewritten in terms of δu, a simple expression for $\overline{(\delta u)^3}/\bar{\epsilon}r$, which is generally interpreted as the energy flux or mean rate of transfer of energy down the cascade at a scale r within the IR, viz.

$$-\frac{\overline{(\delta u)^3}}{\bar{\epsilon}r} = \frac{4}{5}, \tag{1}$$

where the increment $\delta u \equiv u(x + r) - u(x)$ (u is the velocity fluctuation along x, the separation r is along x, and averaging is denoted by an overbar). Equation (1) has become known as the "4/5th" law and is incontrovertibly acknowledged as an exact result for stationary isotropic turbulence when the Reynolds number becomes infinitely large. Further notable contributions in the 1940s were made by Batchelor, mainly through his thorough appraisal of Kolmogorov's theory [5], his monograph on the theory of homogeneous turbulence [6], and his papers with Townsend [7,8] dealing with the transport equation for $\bar{\epsilon}$ (or equivalently the mean enstrophy) in isotropic turbulence and the intermittent nature of the fine-scale structure of turbulence.

Kolmogorov's phenomenology [3], widely known as K41, paved the way to the exciting prospect that small-scale turbulence could be universal, i.e., independent of the Reynolds number and the flow, when the Reynolds number is very large. Kolmogorov postulated that $\bar{\epsilon}$ and the kinematic viscosity ν are the governing parameters for small-scale turbulence. For example, for the velocity structure function, the first similarity hypothesis of K41 predicts that

$$\overline{(\delta u^*)^n} = f_n(r^*), \tag{2}$$

where the asterisk denotes normalization by the Kolmogorov velocity and length scales, $u_K = (\nu\bar{\epsilon})^{1/4}$ and $\eta = (\nu^3/\bar{\epsilon})^{1/4}$, respectively (or equivalently $\bar{\epsilon}$ and ν) and the function f_n is universal. A consequence of Eq. (2) when $r \to 0$ is that the normalized velocity derivative moments should all be constant, i.e., independent of the Taylor microscale Reynolds number $Re_\lambda[\equiv u'\lambda/\nu$, where λ is the longitudinal Taylor microscale $u'/(\partial u/\partial x)'$ and a prime denotes a rms value], viz.

$$S_n = \frac{\overline{(\partial u/\partial x)^n}}{\overline{(\partial u/\partial x)^2}^{n/2}} = \text{const.} \tag{3}$$

Note that S_3 and S_4 are the skewness and flatness factor (or kurtosis) of $\partial u/\partial x$. The second similarity hypothesis of K41 states that, when Re_λ is sufficiently large, the effect of viscosity can be ignored in the IR ($\eta \ll r \ll L$; L is an integral length scale). This leads to the well-known result

$$\overline{(\delta u^*)^n} = C_{un}r^{*n/3}, \tag{4}$$

where C_{un} are "universal" constants. The main outcomes of K41, Eqs. (2)–(4), were completely undermined by the refined hypotheses [9,10] enunciated by Kolmogorov 20 years after K41, hereafter denoted K62.

The refinement, which took into account the so-called spatiotemporal fluctuations in ϵ, assumed a log-normal model for ϵ_r (the subscript r denotes averaging over a volume of linear dimension r), i.e., the probability distribution of $\ln \epsilon_r$ is Gaussian. Two consequences of K62 are as follows: (i) S_n is no longer constant. The magnitude of S_n for $n \geqslant 3$ now increases indefinitely

with Re_λ,

$$|S_n| \sim Re_\lambda^{\beta(n)} \quad (\beta > 0). \tag{5}$$

(ii) Equation (4) now becomes

$$\overline{(\delta u^*)^n} \sim r^{*\zeta_n}, \tag{6}$$

where the exponent ζ_n may depart from $n/3$, except when $n = 3$ [since the "exact" result, Eq. (1), needs to be preserved]. The log-normal and a plethora of subsequent probabilistic models indicate that the departure from $n/3$ increases as n increases, albeit at a rate which can differ between different models. Predictions from physical models, based on generally simplistic proposals of how ϵ is localized in space, have not always qualitatively agreed with Eq. (6) (see for example Sreenivasan and Antonia [11], Wyngaard [12], Van Atta and Antonia [13]). It should be emphasized that, like K41, K62 requires Re_λ to be infinitely large since only in this case can Eq. (1) hold.

It is fair to assert that experimental support for both Eqs. (5) and (6) has been nothing short of considerable. We do not wish to embark on a detailed discussion here; we refer the reader to Refs. [11–14]. Notwithstanding a few notable dissentions, objections, or doubts about K62 (e.g., Refs. [15–19]), the experimental evidence has strongly pointed to K41 having to be abandoned in favor of K62. If we leave aside the results from the atmospheric surface layer (ASL) and recall that perhaps the most "damning" evidence against K41, in the context of Eq. (6), came from the laboratory investigation of Anselmet *et al.* [20], a major criticism that can be levelled at nearly all the laboratory studies is the failure to properly recognize the influence of the Reynolds number on the statistics of velocity derivatives as well as on the moments of δu in the IR, especially since Re_λ has seldom exceeded 1000. It is a fact that the IR has never been observed convincingly due to Re_λ being insufficiently large. For this reason alone, any assertion that the scaling exponent ζ_n is anomalous, i.e., $\zeta_n \neq n/3$, is at the very least questionable, if not meaningless. The realization that the FRN effect has to be taken into account came to the fore in the late 1990s [21–24]. The essence of the approach was to revisit the KH equation (or the Karman-Lin equation [25] in the case of Qian [22] who adopted a spectral approach) which includes the nonstationary term ignored by Kolmogorov [4]. The retention of the nonstationarity permits an assessment of how the large scale inhomogeneity can affect the small scales and hence an estimation of how large Re_λ should be before Eq. (1) is satisfied. Such an estimation was also carried out by Lundgren [26] and Antonia and Burattini [27]. The latter authors showed that "4/5" is approached more rapidly for forced than for decaying turbulence; for a substantial IR to exist, the results indicated that Re_λ may need to exceed 10^3 in the former case and 10^6 in the latter. These results, obtained via a scale-by-scale energy budget, have since been confirmed by Tchoufag *et al.* [28] using the eddy-damped quasi-normal Markovian (EDQNM) method. It seems reasonable to infer that the approach to 4/5 will depend on the flow since the large scales may have different levels of inhomogeneity in different flows.

The above considerations lead to only one conclusion: the previous evidence in support of K62 needs to be critically reappraised in the context of the FRN effect which appears to have been incorrectly mistaken for the intermittency effect. Note that intermittency was not explicitly taken into account in the previously described work since it is intrinsic to the Navier-Stokes (NS) equations. With the benefit of hindsight, the need to account for the intermittency effect in an *ad hoc* fashion, as exemplified by K62, without recourse to the NS equations, seems ludicrous.

The main objective of this paper is to review recent advances in understanding the FRN effect on small-scale quantities such as S_n and $\overline{(\delta u^*)^n}$. In particular, this effect is underpinned by the transport equations for $\overline{(\delta u)^2}$ (or scale-by-scale energy budget) and $\overline{(\delta u)^3}$ (or scale-by-scale budget of local energy-transfer rate), respectively. The limiting forms, at small r, of these budgets have provided valuable insight into the Reynolds number dependence of S_3 and S_4.

II. FRN EFFECT ON THE DR

For homogeneous isotropic turbulence at very large Reynolds number, the transport equation for $\overline{(\delta u)^2}$ is given by

$$-\overline{(\delta u)^3} + 6\nu \frac{\partial}{\partial r}\overline{(\delta u)^2} = \frac{4}{5}\overline{\epsilon}r, \tag{7}$$

which is derived directly from the NS equations. If we divide all terms in Eq. (7) by $\overline{\epsilon}r$, the above relation states, in essence, that the energy flux $-\overline{(\delta u)^3}/\overline{\epsilon}r$ remains constant in the IR [see Eq. (1)]. For small to moderate Reynolds numbers, this equation is usually not satisfied except at small r since Eq. (7) does not contain a large-scale term. For example, Danaila *et al.* [23] showed that Eq. (7) is satisfied only for $r/\eta \leqslant 5$ for grid turbulence at $\mathrm{Re}_\lambda = 66$, suggesting that the large-scale term contributes to Eq. (7) for $r/\eta > 5$. After including such a term, $I_u(r)$ say, Eq. (7) becomes

$$-\overline{(\delta u)^3} + 6\nu \frac{\partial}{\partial r}\overline{(\delta u)^2} = \frac{4}{5}\overline{\epsilon}r - I_u, \tag{8}$$

where I_u may differ from flow to flow. Indeed, different expressions for I_u have been obtained in decaying homogeneous isotropic turbulence (HIT) [23–29], along the axis in the far field of an axisymmetric jet flow [29], and along the centerline of a fully developed channel flow [30]. Equation (8) is of fundamental importance since it is an equilibrium relation between the second- and third-order moments. When $r \to 0$, Eq. (8) reduces to the transport equation for the mean enstrophy or equivalently $\overline{\epsilon}$ (in homogeneous turbulence). This equation can be written in the generic form [29–33],

$$S_3 + 2\frac{G}{\mathrm{Re}_\lambda} = \frac{C}{\mathrm{Re}_\lambda}, \tag{9}$$

where $G \left(=\overline{u^2}\frac{\overline{(\partial^2 u/\partial x^2)^2}}{\overline{(\partial u/\partial x)^2}^2}\right)$ is the enstrophy destruction coefficient and C is a constant which depends on the flow and may vary across regions of the same flow. Equation (9) represents, in essence, a constraint on how S_3 varies with Re_λ in different flows. Since the ratio G/Re_λ approaches a constant relatively rapidly with increasing Re_λ [29–32] and the term on the right side of Eq. (9) must eventually vanish, Eq. (9) implies that the magnitude of S_3 should become constant at sufficiently large Re_λ. This expectation has been confirmed [29–32] and will be discussed briefly in the context of Fig. 1.

Similarly, starting with the NS equations written at two separate and independent spatial points x and x' [or the transport equation for $\overline{(\delta u)^3}$] for HIT, Tang *et al.* [37] and Djenidi *et al.* [38] (see also [39]) derived an expression for S_4, which can be written in a form analogous to Eq. (9), i.e.,

$$S_4 + \gamma = C_1 \frac{S_3}{\mathrm{Re}_\lambda}, \tag{10}$$

where $\gamma [\equiv \gamma_1 \overline{\left(\frac{\partial u^*}{\partial x^*}\right)^2 \left(\frac{\partial^2 p^*}{\partial x^{*2}}\right)}]$; in this expression, p is the pressure fluctuation, γ_1 and C_1 are dimensionless constants). Equation (10) shows that the magnitude of S_4 is balanced by γ, the pressure diffusion of energy term, and the large-scale term $C_1 S_3/\mathrm{Re}_\lambda$; the latter will vanish when Re_λ is sufficiently large. Tang *et al.* [37] and Djenidi *et al.* [38] argued that γ has an upper bound, which implies that S_4 should also be bounded; this is further confirmed by Meldi *et al.* [40] through the eddy-damped quasi-normal Markovian simulation of decaying HIT.

There has been strong support for K41 in the DR from second-order statistics. For example, the Kolmogorov-normalized one-dimensional velocity spectra $\phi_u^*(k_1^*)$ collapse quite well in the high wave-number region [41]. In contrast to the stipulations of K41 and K62, viz., Re_λ must be very large and local isotropy should hold, this collapse does not require Re_λ to be large [42], nor does it require local isotropy to be satisfied rigorously; it does however break down [42] when Re_λ is sufficiently small, typically when it falls below about 40. Pearson and Antonia [43] showed
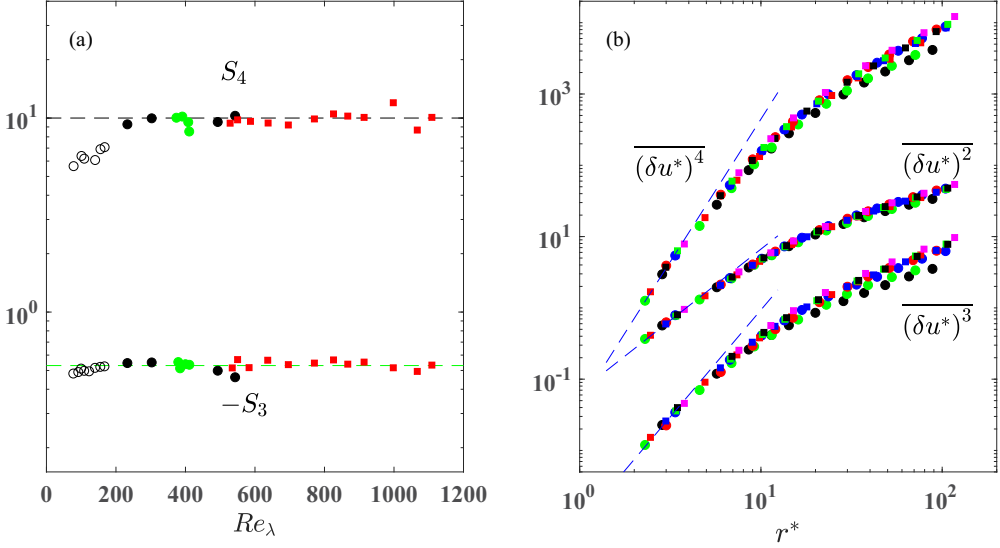
FIG. 1. (a) S_n ($n = 3$ and 4) in a plane jet (■ [32]) and a circular jet (○ [34]; ● [35]; ● [36]). The dashed lines indicate values of S_3 and S_4 averaged over the range $Re_\lambda > 230$. (b) $\overline{(\delta u^*)^n}$ ($n = 2, 3, 4$) in a plane jet [32] for $Re_\lambda = 550$ (■), 696 (■), 826 (■), 914 (■), and 1067 (■) and a circular jet [35] for $Re_\lambda = 235$ (●), 305 (●), 495 (●), and 545 (●); note that S_3 and S_4, as shown in (a), are constant in these two flows for $Re_\lambda > 230$. The blue dashed lines correspond to $15^{-n/2}S_n r^n$ [S_n is the mean value shown in (a)]. Note that $\overline{(\delta u^*)^3}$ has been divided by 10 to avoid interfering with the $\overline{(\delta u^*)^2}$ distributions.

that $\overline{(\delta u^*)^2}$ collapses reasonably well in the DR over a large range of Re_λ ($40 < Re_\lambda < 1175$); Fig. 1(b) confirms this collapse with the use of our data. With reference to Eq. (9), simple analytical expressions can be obtained for C in different flows or for specific regions of a given flow [29–33]. For example, in decaying grid turbulence, $C = \frac{90}{7(1+2R)}(\frac{n+1}{n})$ with $R = \overline{v^2}/\overline{u^2}$, while along the axis in the far field of a round jet, $C = \frac{90}{7(2+R)}$. Since C differs from flow to flow, it is clear that C/Re_λ will approach zero along different paths. Since $2G/Re_\lambda$ becomes constant (≈ 0.53) at $Re_\lambda = 70-100$, we have already shown [29–32] that S_3 depends on both the type of flow and on Re_λ, at small to moderate values of the latter (Fig. 1 of Antonia *et al.* [32]); it will become constant when Re_λ is sufficiently large (in general, Re_λ only needs to exceed about 300, allowing for the uncertainty in measuring S_3). As an example, Fig. 1(a) shows S_3 in plane and circular jets. It can be seen that S_3 is constant when $Re_\lambda > 100$ in these two flows. Consequently, $\overline{(\delta u^*)^3}$ also collapses reasonably well at small r^* [Fig. 1(b)]. For the fourth-order statistics, Fig. 1(a) shows that, in plane and circular jets, S_4 becomes constant beyond $Re_\lambda \approx 300$. This trend is supported by analytical considerations based on the NS equations, as shown above.

However, almost all the previous studies on the evolution of S_3 and S_4 with Re_λ have included the ASL data, e.g., Figs. 5 and 6 of Sreenivasan and Antonia [11], which are reproduced in the insets of Figs. 2(a) and 2(b). A "red" contour has been drawn around the ASL data to distinguish these from the other (laboratory) data. The insets of Figs. 2(a) and 2(b) highlight the impact that the ASL data has had on bolstering the validity of K62 and provide incisive insight into how subsequent researchers may have been misled into accepting, if not wholeheartedly embracing, K62. Admittedly with the benefit of hindsight, the methodology embodied in the insets of Figs. 2(a) and 2(b) can now be criticized on at least three major levels. First, it ignores the FRN effect which can affect the laboratory data in a significant way and, perhaps to a lesser extent, the ASL data. Second, the FRN effect, through its very nature (it mainly reflects the inhomogeneity associated with the large scale motion; the latter has been shown to depend on the flow), is expected to affect
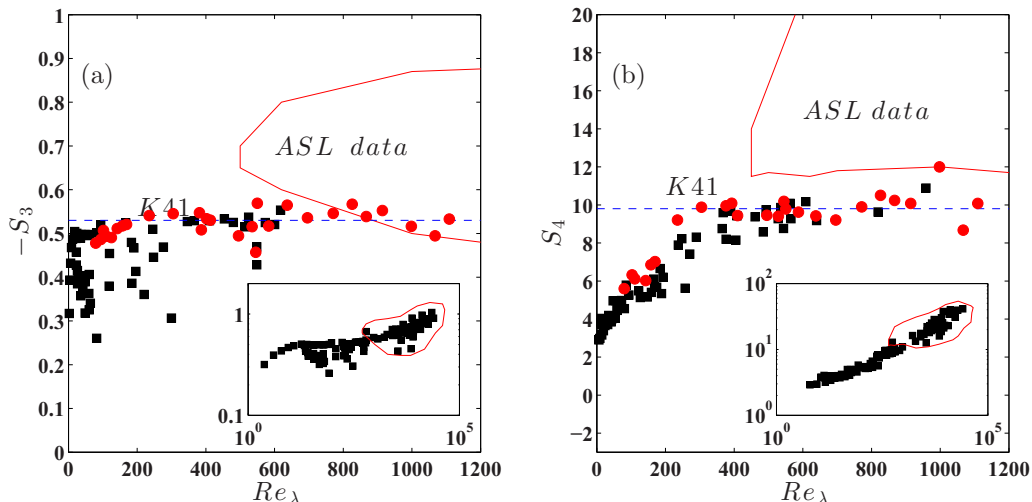
FIG. 2. Laboratory data for S_3 and S_4 reproduced from Figs. 5 and 6 of Sreenivasan and Antonia [11] without identifying the data sources. The insets reproduce all (laboratory and ASL) data from Figs. 5 and 6 of Sreenivasan and Antonia [11]. Note that a "red" contour is drawn around the ASL data to distinguish these from the laboratory data. The data for S_3 and S_4 shown in Fig. 1 are reproduced here (red symbols).

different flows differently. This expectation is completely ignored in the insets of Figs. 2(a) and 2(b), which do indeed show that the laboratory values exhibit "apparent" scatter [our recent work, as discussed above, confirms that, for S_3 and S_4, there is a systematic dependence on Re$_\lambda$ which can be explained analytically, via Eqs. (9) and (10)]. Clearly, one cannot afford to indiscriminately use data obtained from various flows unless the Reynolds number is large enough to allow the FRN effect in each of these flows to be negligible and provided local isotropy is satisfied to a reasonable approximation [recall that Eqs. (7)−(10) rest on this assumption]. The need to achieve a sufficiently high Reynolds number in any given laboratory flow so that the Kolmogorov equation, $[-\overline{(\delta u)^3}/\bar{\epsilon} r = 4/5]$ is satisfied approximately in the IR should, strictly speaking, be considered as a *sine qua non* requirement before examining the consequences of K41 and K62. This seems to have been mostly overlooked. Third, the inclusion of the ASL data when testing K41 and K62 needs, at the very least, to be discussed or scrutinized more objectively than in the past since the ASL data exhibit a strong departure from local homogeneity and local isotropy due to the fact that it is most likely affected by wall-blockage effects and a high mean shear; this has been discussed by Djenidi *et al.* [50] (see also Tang *et al.* [37] in the context of S_4). It is worth recalling Kolmogorov's (1941) comment that "the hypothesis of local isotropy is realized with good approximation in sufficiently small domains...not lying *near the boundary of the flow.*" More importantly, when we disregard the ASL data, the laboratory data in Figs. 2(a) and 2(b) are consistent with the data in Fig. 1, i.e., S_3 and S_4 increase as Re$_\lambda$ increases and eventually become constant when Re$_\lambda$ is sufficiently large. This is precisely in accordance with the NS equations, as expressed by Eqs. (9) and (10) but in disagreement with Eq. (5).

III. FRN EFFECT ON THE IR

We now focus on the FRN effect on the scaling range behavior of various quantities such as the energy spectrum $\phi_u(k_1)$, the pressure spectrum $\phi_p(k_1)$, and the velocity structure functions $\overline{(\delta u)^n}$. The IR is expected to be approximately well developed only when Re$_\lambda$ exceeds a critical value of Re$_\lambda$ which depends on the flow. Figure 3(a) shows the distributions of $\overline{(\delta u^*)^2}$ in various flows (axis
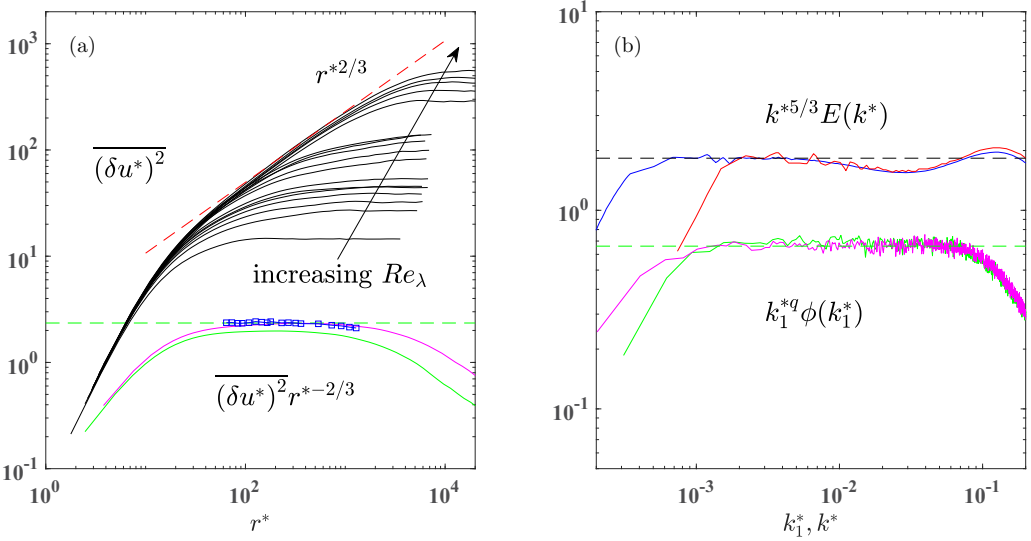
FIG. 3. (a) $\overline{(\delta u^*)^2}$ in grid turbulence [44] ($Re_\lambda = 25-99$), a circular cylinder wake [45] ($Re_\lambda = 160-280$), and a plane jet [46] ($Re_\lambda = 550-1067$). The arrow indicates the direction of increasing Re_λ. Also shown are distributions of $\overline{(\delta u^*)^2}r^{*-2/3}$ for a plane jet [46] ($Re_\lambda = 550$ and 1067, green curve and pink curve, respectively) and a circular jet [47] ($Re_\lambda = 966$, blue square symbols). The green and red dashed lines correspond to 2.35 and $r^{*2/3}$, respectively. (b) Compensated one-dimensional (1D) and 3D energy spectra for DNS (box turbulence) and plane jet data at high Re_λ: pink and green curves correspond to the plane jet data reported in (a); the corresponding exponent q is 1.66 (pink) and 1.61 (green). The blue [48] and red [49] curves correspond to DNS data at $Re_\lambda = 2300$ and 805, respectively. The black and green dashed horizontal lines correspond to 1.83 and 0.66, respectively.

of plane jet, centreline of a circular cylinder wake and grid turbulence) over a large range of Re_λ (=25–1067). Also shown in Fig. 3(a) are the distributions of $\overline{(\delta u^*)^2}r^{*-2/3}$ for plane jet at $Re_\lambda = 550$ and 1067 respectively and circular jet [47] at $Re_\lambda = 966$. We can observe that there is no obvious plateau for $\overline{(\delta u^*)^2}r^{*-2/3}$ at $Re_\lambda = 550$, 966, and 1067, respectively and thus the power-law fit in the scaling range is at best a rough approximation. Clearly, in the light of these results, it should be recognized that the concept of a scaling range, over which $\overline{(\delta u)^n}$ exhibits an approximate power-law dependence on n is strictly untenable. Nonetheless, we have estimated values of the exponents in Eq. (6) using a selection of data, obtained at the University of Newcastle and elsewhere to illustrate our claim that only when the FRN effect disappears can a power-law behavior begin to emerge. We recall that the spectral density $\phi_u^*(k_1^*)$ is more likely to display a scaling range than $\overline{(\delta u^*)^2}$, i.e., the correspondence between these two quantities is also affected by the FRN effect. Figure 3(b) shows the compensated spectra $k_1^{*q}\phi_u^*(k_1^*)$ along the axis of the plane jet at $Re_\lambda = 550$ ($q = 1.61$) and 1067 ($q = 1.66$). Although the two distributions do not exhibit a clear plateau in the scaling range, the Re_λ dependence of q is evident. Also shown in Fig. 3(b) are the compensated 3D spectra $k^{*q}E(k^*)$ for box turbulence DNS data at $Re_\lambda = 805$ and 2300, respectively. There is a restricted wave-number range over which $q \simeq 5/3$. The extent of the plateau increases as Re_λ increases. The variations of ζ_2 and q on Re_λ reported in the literature and our experimental data are shown in Figs. 4(a) and 4(b), respectively. The "2/3" and "−5/3" predictions of K41 are approached slowly as Re_λ increases.

Antonia and Burattini [27] showed that $-\overline{(\delta u)^3}/\bar{\epsilon}r$ approaches 4/5 slowly as Re_λ increases, the approach being relatively more rapid for forced than decaying turbulence [Fig. 4(c)]. Similar results have been obtained [22,24,28] using different types of closures applied to either Eq. (8) or the Karman-Lin spectral equation [25]. Note that only when $I_u(r)$ becomes negligible over a sufficiently
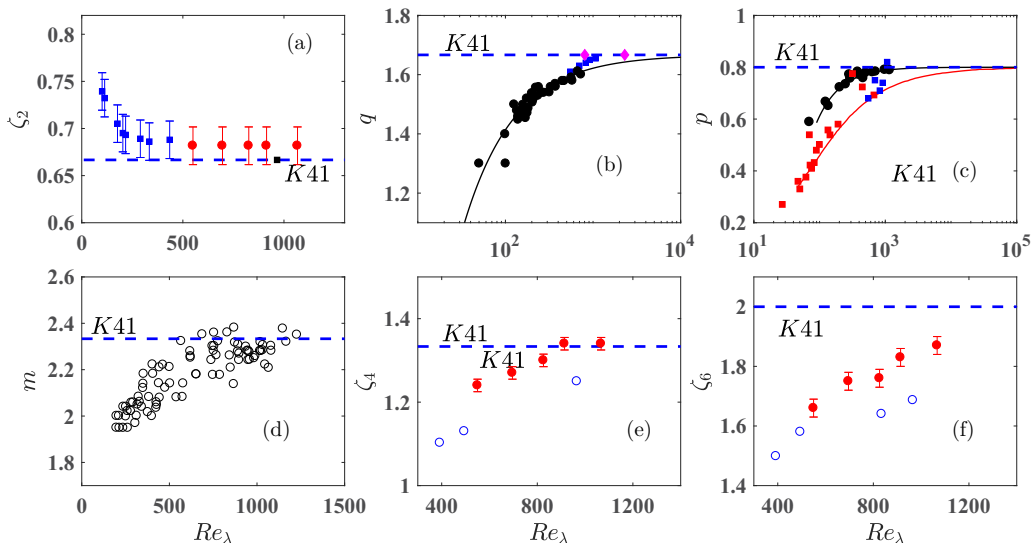
FIG. 4. FRN effect on the scaling range behavior of various quantities in different flows. The dashed horizontal lines correspond to the predictions of K41. Re_λ variation of (a) ζ_2 along the axes of a plane jet (● [46]) and circular jet (■ [47]), and for forced turbulence (■ [51]); (b) $q[\phi_u(k_1) \sim k_1^{-q}]$ in grid turbulence (● [52]) and along the axis of a plane jet (■ [46]); black empirical curve, $q = 5/3 - 8Re_\lambda^{-3/4}$ [52]; (♦), DNS reported in Fig. 3(b); (c) $p = \max[-\overline{(\delta u)^3}/\bar{\epsilon}r]$ in forced turbulence (●, the black curve is a fit to the data) and decaying turbulence (■, the red curve is the analytical prediction [27]; ■, plane jet [46]); (d) $m[\phi_p(k_1) \sim k_1^{-m}]$ along the axis of a circular jet [53]; (e),(f) ζ_4 and ζ_6 [see Eq. (6)] along the axis of a plane jet (●) and circular jet (○) [46].

large range of r can the scaling range be correctly identified with the IR [27]. As an example, we report in Fig. 5 distributions of $\overline{(\delta u^*)^3}/r^*$ in forced turbulence, which approach 4/5 more rapidly than for decaying turbulence [Fig. 4(c)]. Clearly, none of the distributions exhibit an obvious plateau, underlining the absence of an inertial range even for this type of flow at $Re_\lambda \sim 1000$. Strictly, only when Re_λ is sufficiently large for I_u to be negligible over a sufficiently large range of r can Eq. (1) be expected to be valid. One may then reasonably assume that an inertial range is established. We recall that K62 predicts

$$\overline{(\delta u)^2} \sim (\bar{\epsilon}r)^{2/3}(L/r)^{-\mu} \quad \text{or} \quad \overline{(\delta u^*)^2} \sim r^{*2/3}(L/r)^{-\mu}, \tag{11}$$

where L is an "external" length scale, loosely identified here with the integral length scale and μ (denoted by κ in K62) is the intermittency exponent (>0) with a value of typically about 0.2. Taking $r = \lambda$, which is expected to lie near the lower end of the inertial range [27,46,56], and substituting the relation $L/\lambda \sim Re_\lambda$ into (11) lead to $\overline{(\delta u^*)^2}_{r=\lambda} \sim \lambda^{*2/3}Re_\lambda^{-\mu}$ or $\overline{(\delta u^*)^2}_{r=\lambda}/\lambda^{*2/3} \sim Re_\lambda^{-\mu}$. Similarly, from Eq. (1), we can obtain $\overline{(\delta u^*)^3}_{r=\lambda}/\lambda^* = -4/5$. Namely, K62 assumes that $\overline{(\delta u^*)^3}_{r=\lambda}/\lambda^* = -4/5$ is valid and no longer depends on Re_λ but predicts that $\overline{(\delta u^*)^2}_{r=\lambda}/\lambda^{*2/3}$ continues to evolve with Re_λ. This is inconsistent with the close relationship between $\overline{(\delta u)^2}$ and $\overline{(\delta u)^3}$, as required by the NS equations and expressed by Eqs. (7) or (8). It can be inferred from Fig. 3(a) that the magnitude of $\overline{(\delta u^*)^2}$ at $r^* = \lambda^*$ can only increase with Re_λ; the trend of the data does not exclude the possibility of a collapse, consistent with $\overline{(\delta u^*)^2} \sim r^{*2/3}$; note that Eq. (11) is strictly not relevant since the data for $\overline{(\delta u^*)^3}$ are not yet compliant with Eq. (1), as can be inferred from Figs. 4(c) and 5. Several investigations [18,26,51,57] have now shown that $\overline{(\delta u^*)^2} \sim r^{*2/3}$
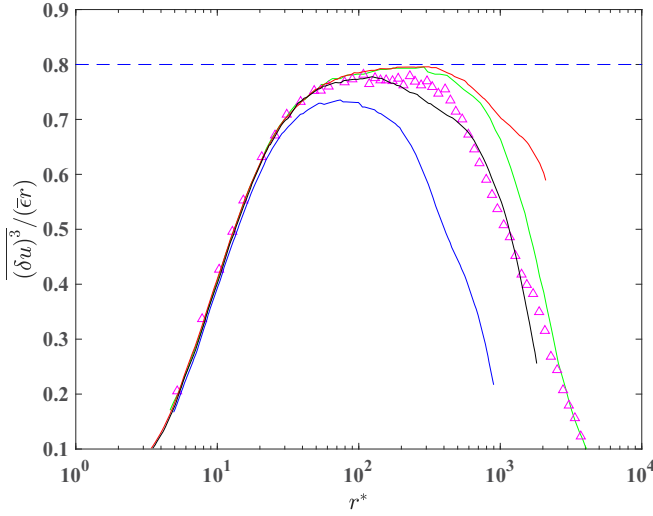
FIG. 5. Distributions of $\overline{(\delta u^*)^3}/r^*$ in forced turbulence. flow between counter-rotating disks at $Re_\lambda = 1170$: $\triangle$ [54]; others are the DNS data (blue, black, and red curves corresponding to $Re_\lambda = 471, 732$, and 1131 respectively [55]; green curve, $Re_\lambda = 805$ [49]). Dashed horizontal line: 4/5.

is the only likely outcome as $Re_\lambda \to \infty$. This may be considered as *a posteriori* justification for Kolmogorov's [4] assumption that the skewness of δu is constant in the inertial range (when $Re_\lambda \to \infty$); Kolmogorov used this assumption to validate the $r^{2/3}$ law, which was derived in [3] using dimensional analysis only.

Tsuji and Ishihara [53] measured the pressure spectrum $\phi_p(k_1)$ on the centerline of a round jet over a large range of Re_λ (=200–1250). A $-7/3$ power-law scaling (K41) for $\phi_p(k_1)$ is approached as Re_λ increases [Fig. 4(d)]. Using EDQNM, Meldi and Sagaut [58] confirmed the FRN effect on the pressure spectrum in decaying homogeneous isotropic turbulence. They indicated that $Re_\lambda \sim 10\,000$ is needed before the pressure spectrum exhibits an IR with an extent of one decade. Tang *et al.* [46] further assessed critically the FRN effect on the scaling range exponents of $\overline{(\delta u)^n}$, with a maximum value of n equal to 8, using experimental and DNS data. In each case, the magnitude of ζ_n increases as Re_λ increases, the rate of increase depending on n. We should emphasize that a power-law variation of $\overline{(\delta u)^n}$, such as given by Eq. (6), is strictly tenable for very large Re_λ; the value of ζ_n is used here only for expedience since the local slope of $\overline{(\delta u)^n}$ does not exhibit a significant plateau. For a fixed Re_λ, the exponent ζ_n can vary from flow to flow and for a given flow, the larger Re_λ is, the closer the exponent is to the K41 value. As an example, Figs. 4(e) and 4(f) show the variations with Re_λ of ζ_4, and ζ_6 along the axes of both plane and circular jets. It is clear from Fig. 4(e) that the 4/3 power-law scaling (K41) for $\overline{(\delta u)^4}$ appears to have been reached for $Re_\lambda > 900$, whereas at the highest Re_λ (=1067), ζ_6 is still noticeably smaller than the K41 value of 2.

Finally, although there may be some differences between the behavior of the velocity field and that of the passive scalar field, it is worth mentioning that there is also a FRN effect (if the Prandtl number is close to 1, the FRN effect is equivalent to a finite Peclet number effect) on the small-scale quantities associated with a passive scalar field such as the skewness S_T ($\equiv \frac{\overline{(\partial u/\partial x)(\partial \theta/\partial x)^2}}{\overline{(\partial u/\partial x)^2}^{1/2}\,\overline{(\partial \theta/\partial x)^2}}$) of the mixed velocity derivative-temperature derivative (θ is the instantaneous temperature fluctuation), and $\overline{(\delta \theta)^n}$. Indeed, Tang *et al.* [59] derived an expression for S_T similar to Eq. (9) for HIT from the generalized Yaglom's equation [23]. The available data for S_T in HIT show that the magnitude of S_T approaches a constant as the Reynolds number increases. Further, since the FRN effect disappears very slowly with increasing Reynolds number, we expect that if one assumes $\overline{(\delta \theta)^n} \sim r^{\alpha_{\theta n}}$ in the

scaling range, then, like ζ_n, $\alpha_{\theta n}$ is likely to be affected by the nonhomogeneity and anisotropy of the large scales. For example, DNS results of box turbulence [60] at $\mathrm{Re}_\lambda \sim 400$ show that the uniform mean scalar gradient can affect $\alpha_{\theta n}$ significantly. Experimental evidence [61,62] also show that $\alpha_{\theta n}$ strongly depends on the scalar injection mechanism, i.e., the initial conditions, in the wake of a circular cylinder at $\mathrm{Re}_\lambda = 370$. Evidently, as for ζ_n, much higher values of Re_λ are needed before the FRN effect on $\alpha_{\theta n}$ disappears.

IV. CONCLUDING DISCUSSION

K41 and K62 require Re_λ to be large. But what exactly is "large"? The results in Secs. II and III suggest that this threshold value of Re_λ, $(\mathrm{Re}_\lambda)_{th}$ say, may differ from flow to flow and, for a given flow, may depend on the initial conditions and the specific quantity investigated. For example, for higher-order velocity structure functions in the scaling range, $(\mathrm{Re}_\lambda)_{th} \geqslant 10^5$–$10^6$ whereas for S_3 and S_4, $(\mathrm{Re}_\lambda)_{th} \leqslant 10^3$. In summary, the need to first account for the FRN effect is paramount; in particular, intermittency, as measured for example by S_4, evolves with Re_λ until $(\mathrm{Re}_\lambda)_{th}$ is reached. Since it does not change beyond this threshold, it cannot be responsible for any modifications to K41. This strongly suggests that K62, at least in the way it has been generally interpreted in the literature, is based on a false premise.

The present NS based analytical considerations, together with the experimental evidence (Figs. 1–4), strongly imply that the intermittency model proposed by Kolmogorov (K62) and subsequent intermittency models are, at best, *ad hoc* attempts to model the FRN effect. Further, they seem to support an approach towards K41 as Re_λ continues to increase. Evidently, more high quality data, preferably for Re_λ in excess of 1000, are needed to further confirm this tendency towards K41. It would seem, as highlighted by the unmistakable trend of the data in Fig. 4, that our quest for a universal, or at least quasi-universal, state for small-scale turbulence may not be unreasonable after all.

ACKNOWLEDGMENTS

[1] G. I. Taylor, Statistical theory of turbulence, Proc. R. Soc. London, Ser. A **151**, 421 (1935).

[2] T. Von Kármán and L. Howarth, On the statistical theory of isotropic turbulence, Proc. R. Soc. London, Ser. A **164**, 192 (1938).

[3] A. N. Kolmogorov, The locally structure of turbulence in incompressible viscous fluid for very large Reynolds numbers, Dokl. Akad. Nauk SSSR **30**, 299 (1941); see also Proc. R. Soc. London, Ser. A **434**, 9 (1991).

[4] A. N. Kolmogorov, Dissipation of energy in the locally isotropic turbulence, Dokl. Akad. Nauk SSSR **32**, 19 (1941); see also Proc. R. Soc. London, Ser. A **434**, 15 (1991).

[5] G. K. Batchelor, Kolmogoroff's theory of locally isotropic turbulence, Math. Proc. Cambridge Philos. Soc. **43**, 533 (1947).

[6] G. K. Batchelor, *The Theory of Homogeneous Turbulence* (Cambridge University Press, Cambridge, UK, 1953).

[7] G. K. Batchelor and A. A. Townsend, Decay of vorticity in isotropic turbulence, Proc. R. Soc. London, Ser. A **190**, 534 (1947).

[8] G. K. Batchelor and A. A. Townsend, The nature of turbulent motion at large wave-numbers, Proc. R. Soc. London, Ser. A **199**, 238 (1949).

[9] A. N. Kolmogorov, A refinement of previous hypotheses concerning the local structure of turbulence in a viscous incompressible fluid at high Reynolds number, J. Fluid Mech. **13**, 82 (1962).

[10] A. M. Oboukhov, Some specific features of atmospheric turbulence, J. Fluid Mech. **13**, 77 (1962).

[11] K. Sreenivasan and R. A. Antonia, The phenomenology of small-scale turbulence, Annu. Rev. Fluid Mech. **29**, 435 (1997).

[12] J. C. Wyngaard, *Turbulence in the Atmosphere* (Cambridge University Press, Cambridge, UK, 2010).

[13] C. W. Van Atta and R. A. Antonia, Reynolds number dependence of skewness and flatness factors of turbulent velocity derivatives, Phys. Fluids **23**, 252 (1980).

[14] F. Anselmet, R. A. Antonia, and L. Danaila, Turbulent flows and intermittency in laboratory experiments, Planet. Space Sci. **49**, 1177 (2001).

[15] U. Frisch, *Turbulence: The Legacy of AN Kolmogorov* (Cambridge University Press, Cambridge, UK, 1995).

[16] J. Qian, Skewness factor of turbulent velocity derivative, Acta Mech. Sin. **10**, 12 (1994).

[17] S. Grossmann and D. Lohse, Scale resolved intermittency in turbulence, Phys. Fluids **6**, 611 (1994).

[18] J. Qian, Normal and anomalous scaling of turbulence, Phys. Rev. E **58**, 7325 (1998).

[19] W. D. McComb, *Homogeneous, Isotropic Turbulence: Phenomenology, Renormalization and Statistical Closures* (Oxford University Press, Oxford, 2014).

[20] Anselmet, Y. Gagne, E. J. Hopfinger, and R. A. Antonia, Higher-order velocity structure functions in turbulent shear flows, J. Fluid Mech. **140**, 63 (1984).

[21] J. Qian, Inertial range and the finite Reynolds number effect of turbulence, Phys. Rev. E **55**, 337 (1997).

[22] J. Qian, Slow decay of the finite Reynolds number effect of turbulence, Phys. Rev. E **60**, 3409 (1999).

[23] L. Danaila, F. Anselmet, T. Zhou, and R. A. Antonia, A generalization of Yaglom's equation which accounts for the large-scale forcing in heated decaying turbulence, J. Fluid Mech. **391**, 359 (1999).

[24] E. Lindborg, Correction to the four-fifths law due to variations of the dissipation, Phys. Fluids **11**, 510 (1999).

[25] T. Von Karman and C. C. Lin, On the concept of similiarity in the theory of isotropic turbulence, Rev. Mod. Phys. **21**, 516 (1949).

[26] T. S. Lundgren, Kolmogorov turbulence by matched asymptotic expansions, Phys. Fluids **15**, 1074 (2003).

[27] R. A. Antonia and P. Burattini, Approach to the 4/5 law in homogeneous isotropic turbulence, J. Fluid Mech. **550**, 175 (2006).

[28] J. Tchoufag, P. Sagaut, and C. Cambon, Spectral approach to finite Reynolds number effects on Kolmogorov's 4/5 law in isotropic turbulence, Phys. Fluids **24**, 015107 (2012).

[29] R. A. Antonia, S. L. Tang, L. Djenidi, and L. Danaila, Boundedness of the velocity derivative skewness in various turbulent flows, J. Fluid Mech. **781**, 727 (2015).

[30] S. L. Tang, R. A. Antonia, L. Djenidi, H. Abe, T. Zhou, L. Danaila, and Y. Zhou, Transport equation for the mean turbulent energy dissipation rate on the centreline of a fully developed channel flow, J. Fluid Mech. **777**, 151 (2015).

[31] S. L. Tang, R. A. Antonia, L. Djenidi, and Y. Zhou, Transport equation for the mean turbulent energy dissipation rate in the far-wake of a circular cylinder, J. Fluid Mech. **784**, 109 (2015).

[32] R. A. Antonia, L. Djenidi, L. Danaila, and S. L. Tang, Small scale turbulence and the finite Reynolds number effect, Phys. Fluids **29**, 020715 (2017).

[33] F. Thiesset, R. A. Antonia, and L. Djenidi, Consequences of self-preservation on the axis of a turbulent round jet, J. Fluid Mech. **748**, R2 (2014).

[34] J. Mi, M. Xu, and T. Zhou, Reynolds number influence on statistical behaviors of turbulence in a circular free jet, Phys. Fluids **25**, 075101 (2013).

[35] G. Xu, R. A. Antonia, and S. Rajagopalan, Sweeping decorrelation hypothesis in a turbulent round jet, Fluid Dyn. Res. **28**, 311 (2001).

[36] R. A. Antonia, B. R. Satyaprakash, and A. K. M. F. Hussain, Statistics of fine-scale velocity in turbulent plane and circular jets, J. Fluid Mech. **119**, 55 (1982).

[37] S. L. Tang, R. A. Antonia, L. Djenidi, and Y. Zhou, Reappraisal of the velocity derivative flatness factor in various turbulent flows, J. Fluid Mech. **847**, 244 (2018).

[38] L. Djenidi, L. Danaila, R. A. Antonia, and S. Tang, A note on the velocity derivative flatness factor in decaying HIT, Phys. Fluids **29**, 051702 (2017).

[39] L. Djenidi, R. A. Antonia, and S. L. Tang, Scale-invariance in finite Reynolds number homogeneous isotropic turbulence, J. Fluid Mech. **864**, 244 (2019).

[40] M. Meldi, L. Djenidi, and R. A. Antonia, Reynolds number effect on the velocity derivative flatness factor, J. Fluid Mech. **856**, 426 (2018).

[41] R. A. Antonia, L. Djenidi, and L. Danaila, Collapse of the turbulent dissipation range on Kolmogorov scales, Phys. Fluids **26**, 045105 (2014).

[42] L. Djenidi, S. F. Tardu, R. A. Antonia, and L. Danaila, Breakdown of Kolmogorov's first similarity hypothesis in grid turbulence, J. Turbul. **15**, 596 (2014).

[43] B. R. Pearson and R. A. Antonia, Reynolds-number dependence of turbulent velocity and pressure increments, J. Fluid Mech. **444**, 343 (2001).

[44] T. Zhou and R. A. Antonia, Reynolds number dependence of the small-scale structure of grid turbulence, J. Fluid Mech. **406**, 81 (2000).

[45] R. A. Antonia, T. Zhou, and G. P. Romano, Small-scale turbulence characteristics of two-dimensional bluff body wakes, J. Fluid Mech. **459**, 67 (2002).

[46] S. L. Tang, R. A. Antonia, L. Djenidi, L. Danaila, and Y. Zhou, Finite Reynolds number effect on the scaling range behavior of turbulent longitudinal velocity structure functions, J. Fluid Mech. **820**, 341 (2017).

[47] R. A. Antonia, B. R. Satyaprakash, and A. J. Chambers, Reynolds number dependence of velocity structure functions in turbulent shear flows, Phys. Fluids **25**, 29 (1982).

[48] T. Ishihara, K. Morishita, M. Yokokawa, A. Uno, and Y. Kaneda, Energy spectrum in high-resolution direct numerical simulations of turbulence, Phys. Rev. Fluids **1**, 082403(R) (2016).

[49] T. Gotoh and T. Watanabe, Power and Nonpower Laws of Passive Scalar Moments Convected by Isotropic Turbulence, Phys. Rev. Lett. **115**, 114502 (2015).

[50] L. Djenidi, R. A. Antonia, M. K. Talluru, and H. Abe, Skewness and flatness factors of the longitudinal velocity derivative in wall-bounded flows, Phys. Rev. Fluids **2**, 064608 (2017).

[51] W. D. McComb, S. R. Yoffe, M. F. Linkmann, and A. Berera, Spectral analysis of structure functions and their scaling exponents in forced isotropic turbulence, Phys. Rev. E **90**, 053010 (2014).

[52] L. Mydlarski and Z. Warhaft, Passive scalar statistics in high-Peclet-number grid turbulence, J. Fluid Mech. **358**, 135 (1998).

[53] Y. Tsuji and T. Ishihara, Similarity scaling of pressure fluctuation in turbulence, Phys. Rev. E **68**, 026309 (2003).

[54] F. Moisy, P. Tabeling, and H. Willaime, Kolmogorov Equation in a Fully Developed Turbulence Experiment, Phys. Rev. Lett. **82**, 3994 (1999).

[55] T. Ishihara, T. Gotoh, and Y. Kaneda, Study of high-Reynolds number isotropic turbulence by direct numerical simulation, Annu. Rev. Fluid Mech. **41**, 165 (2009).

[56] J. Boschung, M. Gauding, F. Hennig, D. Denker, and H. Pitsch, Finite Reynolds number corrections of the 4/5 law for decaying turbulence, Phys. Rev. Fluids **1**, 064403 (2016).

[57] J. Qian, Closure Approach to High-Order Structure Functions of Turbulence, Phys. Rev. Lett. **84**, 646 (2000).

[58] M. Meldi and P. Sagaut, Further insights into self-similarity and self-preservation in freely decaying isotropic turbulence, J. Turbul. **14**, 24 (2013).

[59] S. L. Tang, R. A. Antonia, L. Djenidi, L. Danaila, and Y. Zhou, Boundedness of the mixed velocity-temperature derivative skewness in homogeneous isotropic turbulence, Phys. Fluids **28**, 095102 (2016).

[60] T. Watanabe and T. Gotoh, Intermittency in passive scalar turbulence under the uniform mean scalar gradient, Phys. Fluids **18**, 058105 (2006).

[61] J. Lepore and L. Mydlarski, Effect of the Scalar Injection Mechanism on Passive Scalar Structure Functions in a Turbulent Flow, Phys. Rev. Lett. **103**, 034501 (2009).

[62] J. Lepore and L. Mydlarski, Finite Peclet number effects on the scaling exponents of high order passive scalar structure functions, J. Fluid Mech. **713**, 453 (2012).